PROCEEDINGS OF THE ROYAL SOCIETY B

rspb.royalsocietypublishing.org

Research

**Cite this article:** Schwager H, Masselter T, Speck T, Neinhuis C. 2013 Functional morphology and biomechanics of branch–stem junctions in columnar cacti. Proc R Soc B 280: 20132244.
http://dx.doi.org/10.1098/rspb.2013.2244

Received: 4 September 2013
Accepted: 24 September 2013

**Subject Areas:**
biomechanics, plant science

**Keywords:**
columnar cacti, functional anatomy, branching, finite-element analysis, biomimetics

**Author for correspondence:**
Hannes Schwager
e-mail: hannes.schwager@tu-dresden.de

Electronic supplementary material is available at http://dx.doi.org/10.1098/rspb.2013.2244 or via http://rspb.royalsocietypublishing.org.

Royal Society Publishing
Informing the science of the future



# Functional morphology and biomechanics of branch–stem junctions in columnar cacti

Hannes Schwager[1], Tom Masselter[2], Thomas Speck[2] and Christoph Neinhuis[1]

[1]Institute for Botany, Botanic Garden, Faculty of Science, Technische Universität Dresden, Zellescher Weg 20b, 01062 Dresden, Germany
[2]Plant Biomechanics Group, Botanic Garden, Faculty of Biology, University of Freiburg, Schänzlestraße 1, 79104 Freiburg, Germany

Branching in columnar cacti features morphological and anatomical characteristics specific to the subfamily Cactoideae. The most conspicuous features are the pronounced constrictions at the branch–stem junctions, which are also present in the lignified vascular structures within the succulent cortex. Based on finite-element analyses of ramification models, we demonstrate that these indentations in the region of high flexural and torsional stresses are not regions of structural weakness (e.g. allowing vegetative propagation). On the contrary, they can be regarded as anatomical adaptations to increase the stability by fine-tuning the stress state and stress directions in the junction along prevalent fibre directions. Biomimetic adaptations improving the functionality of ramifications in technical components, inspired, in particular, by the fine-tuned geometrical shape and arrangement of lignified strengthening tissues of biological role models, might contribute to the development of alternative concepts for branched fibre-reinforced composite structures within a limited design space.

## 1. Introduction

As an adaptation to arid or semi-arid habitats, columnar cacti evolved differently from most other dicotyledonous plants. The two most conspicuous morphological characteristics are spine-wearing areoles and the succulent cortex [1]. In contrast to the widely accepted constructional principle stating that supporting tissues should be arranged in the periphery of erect columnar or tubular structures to increase the bending stiffness and the safety against buckling by increasing the respective axial second moment of area [2], the lignified vascular (supporting) tissue in cacti shoots is located more centrally. Succulent cortical tissues for water storage, assimilation and transpiration surround a tube of conducting tissue and fibres (figure 1*d–f*) [3]. It has been demonstrated that this succulent cortex compensates (at least partly) for the mechanically 'disadvantageous' arrangement of the cactus wood in younger (apical) parts of cactus shoots [4].

The distinct constriction of their ramifications at the branching points owing to the presence of the succulent cortex is another morphological peculiarity of columnar cacti and has not been subject of biomechanical analyses yet. Prior investigations on the stability of branching in plants mainly focused on tree ramifications that do not show such constrictions. For these 'normal' ramifications, the main consensus is that specific load adaptation strategies lead to homogeneous stress–strain conditions in the branching region [5–8]. Typically, the basal diameter of a tree branch is correlated with the acting bending moment caused by its dead weight and additional wind loads [9]. The transition zone between stem and branch exhibits a special outer contour, avoiding notch stress concentrations near the surface. This helps to minimize the risk of failure owing to crack initiation and propagation [5,10,11].

In apparent contradiction to this theory of uniform stress distribution are the neckings found at the point of branching in columnar cacti (figure 2*a–c*). Owing

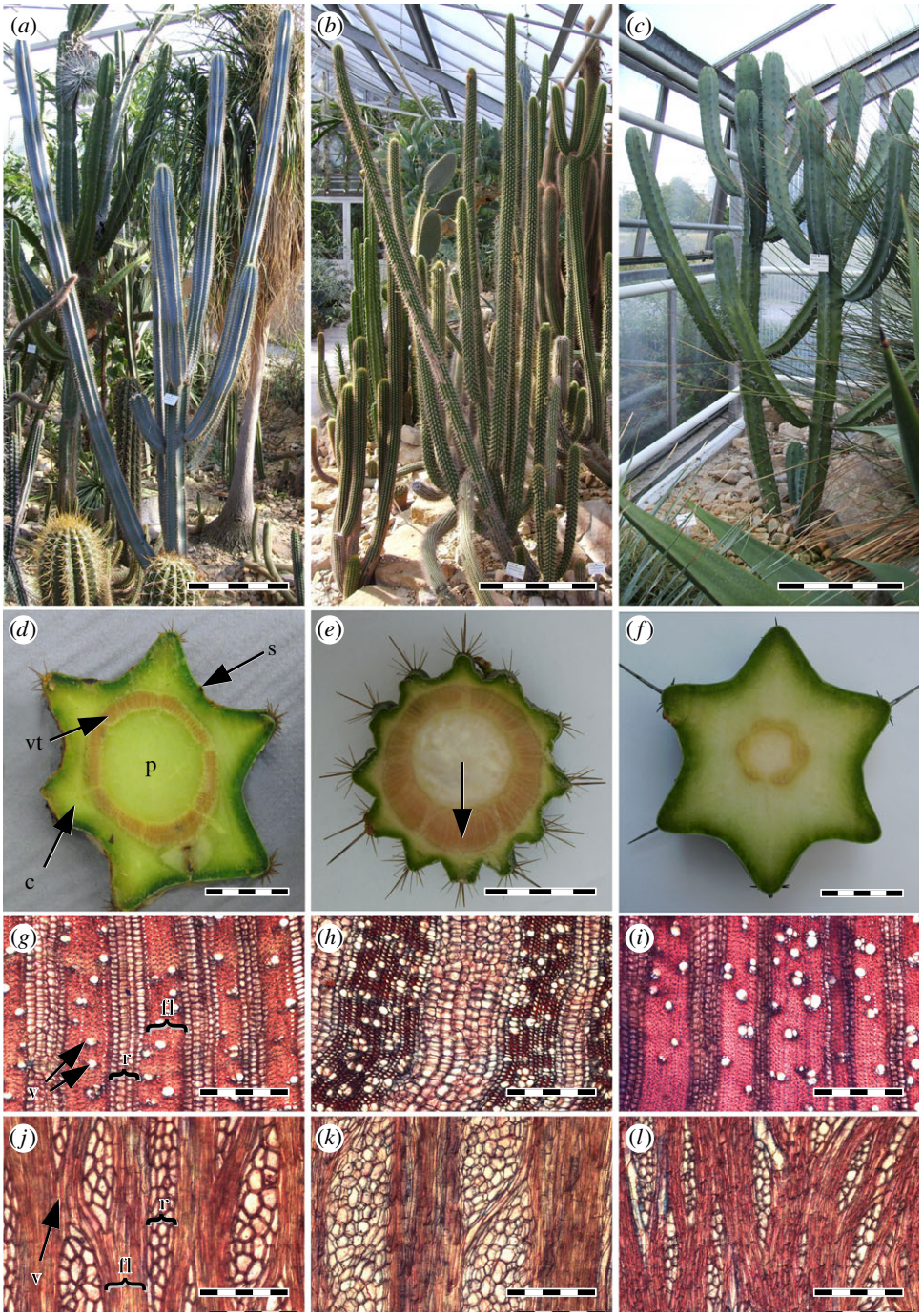


**Figure 1.** *Pilosocereus pachycladus*: (*a*) whole plant; (*d*) cross-section of a branch; (*g*) wood in cross section; (*j*) wood in longitudinal tangential section. *Cleistocactus morawetzianus*: (*b*) whole plant; (*e*) cross-section of a branch; (*h*) wood in cross section; (*k*) wood in longitudinal tangential section. *Myrtillocactus geometrizans*: (*c*) whole plant; (*f*) cross section of a branch; (*i*) wood in cross section; (*l*) wood in longitudinal tangential section. Scale bars: (*a–c*) 50 cm; (*d–f*) 25 mm; (*g–l*) 500 µm. s, skin; c, cortex; vt, lignified vascular tissue (cactus wood); p, pith; fl, fibre lamella; v, vessel; r, ray.

to the smaller diameter, the axial second moment of area and the polar second moment of area of the branch are decreased at the junction (i.e. in this region, the extent of geometrical influence on the resistance to bending and torsion is reduced). From an engineering point of view, the construction is not well adapted to the predominant loading conditions. Assuming that the ramifications represent no predetermined breaking points for vegetative propagation, as proved for some prickly pear species [12], the load adaptation has to be accomplished by the inner structure of the lignified tissues.

The aim of our study is to examine the stability and the integrity of ramifications in three species of columnar cacti (*Pilosocereus pachycladus*, *Cleistocactus morawetzianus* and *Myrtillocactus geometrizans*). A special focus is on the mechanical interaction between the inner fibre arrangement of the vascular tissue in combination with the presence of the succulent cortex and the shape of the junction. Our results suggest a cactus-specific load adaptation strategy.

## 2. Material and methods

### (a) Material

Individuals of *P. pachycladus* Ritt., *C. morawetzianus* Backeb. and *M. geometrizans* Mart. were cultivated and collected in the Botanic Garden of the Technische Universität Dresden. All specimens

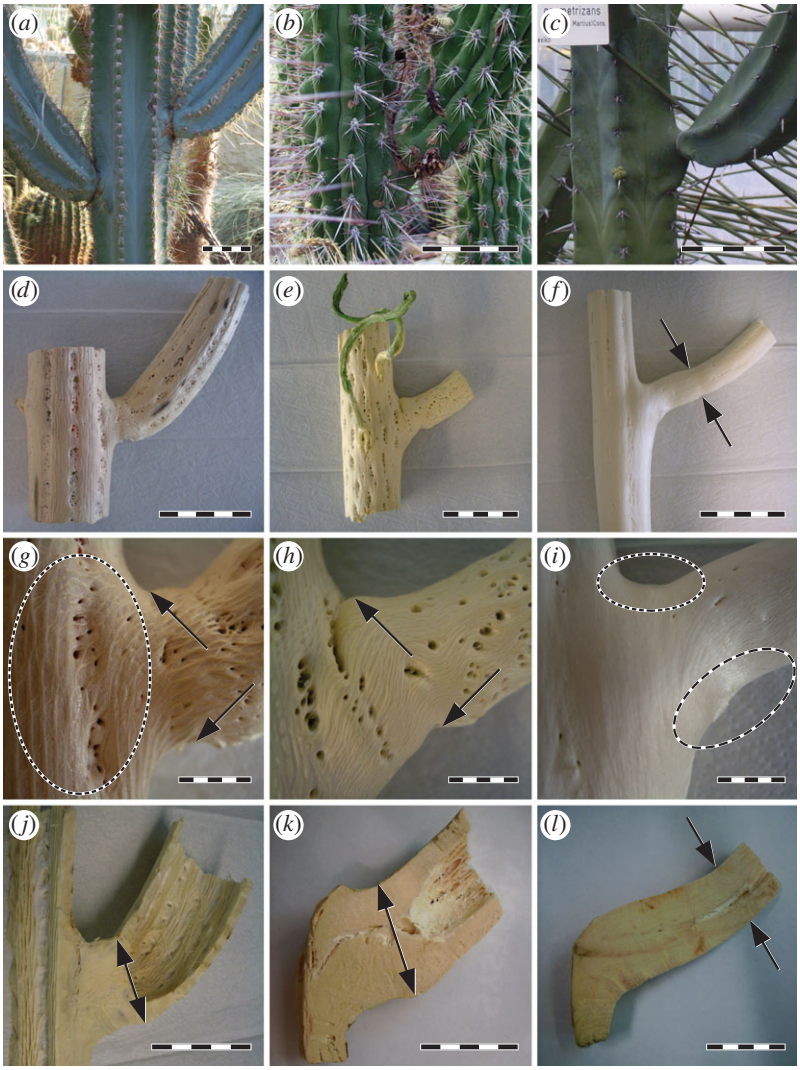


**Figure 2.** *Pilosocereus pachycladus*: (*a*) Entire ramification; (*d*) isolated wood cylinder of the ramification; (*g*) stem branch junction; (*j*) median longitudinal section of the attachment zone. *Cleistocactus morawetzianus*: (*b*) entire ramification; (*e*) isolated wood cylinder of the ramification; (*h*) stem branch junction; (*k*) median longitudinal section of the attachment zone. *Myrtillocactus geometrizans*: (*c*) entire ramification; (*f*) isolated wood cylinder of the ramification; (*i*) stem branch junction; (*l*) median longitudinal section of the attachment zone. Scale bars: (*a,c*) 10 cm; (*b*) 5 cm; (*d–f*) 10 cm; (*g–i*) 10 mm; (*j–l*) 25 mm. Arrows: (*f,j–l*) passageway of the vascular tissue through the epidermis; (*g,h*) indentations on adaxial and abaxial side of the stem branch junction (*P. pachycladus* and *C. morawetzianus*). Dotted circle: (*g*) lateral region of high cross-linkage between the fibre lamellae (*P. pachycladus*); (*i*) missing indentations (*M. geometrizans*).

were planted in greenhouses with seasonal irrigation in summer (i.e. they were not exposed to wind or abnormal long periods of drought).

*Pilosocereus pachycladus* (figures 1*a*,*d*,*g*,*j* and 2*a*,*d*,*g*,*j*) is a shrubby to tree-like species originating from northeastern Brazil [13,14] where the wet season lasts from November to January. The investigated specimen was tree-like. The well-defined, erect trunk reached a total height of 5 m and 12 cm in diameter at stem base. The branches originated 1.5 m aboveground and attained diameters of up to 11 cm (figure 1*a*).

*Cleistocactus morawetzianus* (figures 1*b*,*e*,*h*,*k* and 2*b*,*e*,*h*,*k*) is a shrubby cactus from central Peru [13,14], native in regions with a distinctive seasonality. The area of origin is subjected to heavy precipitation in December and January, and extreme drought from May to September. The shoots of the investigated individual grew up to 2.5 m in height and 5 cm in diameter. Occasional branching appeared only near the base (figure 1*b*).

*Myrtillocactus geometrizans* (figures 1*c*,*f*,*i*,*l* and 2*c*,*f*,*i*,*l*) is a tree-like cactus from Mexico typically with a short trunk and numerous upcurving branches [13,14]. The investigated plant reached 2.5 m in height and showed a candelabra-like branching with basally tapered side shoots and maximum shoot diameters of 10 cm (figure 1*c*).

## (b) Anatomical investigations

For macroscopic studies, the specimens were dissected manually, and the lignified tissues of the ramifications were prepared by enzymatic maceration with cellulase and pectinase at 37°C. The enzyme solution was buffered with citric acid (pH 5.5), stabilized with polyvinylpyrrolidone and conserved with sodium azide. The fibre course in the ramification zone was determined by analysing macroscopic lateral views, median longitudinal and transverse sections with the digital image processing software ImageJ v. 1.47t.

The microscopic investigations focused on the cactus wood. Transverse, radial and tangential thin sections were prepared on a sliding microtome (Modell 1120, Jung AG) and stained with Safranin–Astrablue.

## (c) Material tests

The mechanical properties of the four main tissues (skin—consisting of cuticle, epidermis and collenchymatous hypodermis; cortex—consisting of chlorenchyma and hydrenchyma; wood—consisting of fibres, vessels and rays; and pith—consisting of storage parenchyma) were determined in quasi-static mechanical

tests performed with specimens cut from non-ramified cactus segments using a Zwicki-Line 2.5 kN material testing machine (Zwick GmbH & Co. KG, Germany) [15]. For details of the sample preparation and the test methods, compare with electronic supplementary material, material test: procedures.

### (d) Biomechanical modelling with finite-element analysis

Three-dimensional computer models of the cactus ramifications were generated with the finite-element modelling software PATRAN v. 2012 (MSC Software Corp.). The results of the described anatomical and mechanical investigations served as input parameters for these models. Particular care was paid to represent correctly the morphological and anatomical characteristics of the investigated species. For details of the modelling, compare with electronic supplementary material, biomechanical modelling.

The finite-element software suite ABAQUS v. 6.6.1 (Dassault Systèmes) was used for the numerical analyses of the generated models. As the stability of a structure always depends on the constituent material as well as its geometry, several simulation runs with variation in these parameters were performed. Results of entire ramification models were compared with simulations taking only the vascular tissue and the pith into account to clarify the mechanical role of the succulent cortex. Models with orthotropic and isotropic material constants were used to highlight the influence of the fibrous wood on the stress state in the ramification zone. The results of these simulations (*P. pachycladus*: figure 4*e*,*i*; *M. geometrizans*: figure 4*f*,*j*) were compared with a simple reference model consisting of two joint cylindrical tubes (figure 4*c*,*g*) as well as a biomimetically optimized model using the design rules established by Mattheck for mimicking tree ramifications (figure 4*d*,*h*) [5,10,11].

## 3. Results

### (a) Anatomy

#### (i) *Pilosocereus pachycladus*

In cross-sections of the trunk or the side shoots, the arrangement of the four main tissues (pith, cortex, wood and skin) of *P. pachycladus* (figure 1*a*) is radially symmetric. The shape of the cortex resembles a regular star polygon with six ribs in the form of equilateral triangles (figure 1*d*). The wood tube has a central position within the erect stem. It is tangentially segmented into loosely interconnected wood strands by the axially superimposed lacunae underneath the areoles on the ribs' crest (figure 2*d*). The wood strands consist of an alternating sequence of axially and radially straight fibre lamellae and parenchymatous rays (figure 1*g*,*j*).

The wood strands in the stem below a ramification adjacent to the branching point are thickened. Their vascular tissue partly diverges out in radial direction, forming a compact socket inside the succulent cortex (figure 2*j*). In cross-section, this socket is of elliptical shape with major axis in transversal direction. After passing through the epidermis (arrows in figure 2*j*), the vascular tissue is enlarged in diameter, forming the above-described wood tube filled with parenchymatous pith (figure 2*a*,*d*,*j*). Remarkable anatomic details are distinct indentations on the adaxial and abaxial side of the elliptical socket at the transition to the vascular tissue of the stem (arrows in figure 2*g*). The fibres originating in the wood strands of the stem circumvent the indentations and join on the adaxial and abaxial side of the socket. In the indented area on the abaxial side, no privileged fibre direction is prevalent. In the stem, adjacent to the branch base, an increased number of interconnections towards the branch base are visible between the axially running fibre lamellae (dotted circle in figure 2*g*).

#### (ii) *Cleistocactus morawetzianus*

The long slender branches of *C. morawetzianus* (figure 1*b*) form a wide upward curve. In periods of drought, the shoots become limp and bend down. In cross-section, the vascular tube is developed eccentrically towards the adaxial side of the branch, resulting in a thickened tube wall on the abaxial side (arrow in figure 1*e*). The vascular tube has an elliptical form with major axis arranged in transversal direction. Most of the adjacent cortex parenchyma is of firm consistency. A continuous tangential segmentation of the vascular tube into distinct straight wood strands is lacking. The lacunae are superimposed with an alternating offset leading to a netlike structure of the tube wall (figure 2*e*) and a meandering course of the wood strands in longitudinal direction. In radial direction, the lamellae exhibit a meandering shape (figure 1*h*). Horizontal growth ruptures subdivide the pith within the shoots.

The ramifications of *C. morawetzianus* feature the same anatomical details as *P. pachycladus*: the vascular tube of the stem beneath the branching is thickened. A compact socket of elliptical cross-section with transversal major axis forms the junction between the vascular tissues of branch and the vascular tissue of the stem (figure 2*k*). Distinct indentations on the adaxial and abaxial side exist (arrows in figure 2*h*).

#### (iii) *Myrtillocactus geometrizans*

The investigated specimens of *M. geometrizans* (figure 1*c*) differ significantly in some anatomical aspects from the species described above: the cortex is much thicker, resulting in a comparatively small central vascular tube (figure 1*f*). The distance between the areoles is larger, and the vascular tube forms an almost closed wall with hardly visible lacunae (figure 2*f*). The fibres run straight in longitudinal direction. The rays are small and dispersed (figure 1*l*). The shape of the wood lamellae in radial direction is also straight, and the fibres exhibit very thick, lignified cell walls (figure 1*i*).

The shape of the vascular tissue in the ramification with its smooth contours resembles a typical deciduous tree ramification (figure 2*f*). The outer diameter of the vascular tissue does not expand after passing through the epidermis. Only a slight necking at the passageway through the epidermis can be found (arrows in figure 2*f*). No distinct indentations such as in *P. pachycladus* and *C. morawetzianus* are present at the junction between branch and stem (compare dotted circles in figure 2*i* with arrows in figure 2*g*,*h*). On the other hand, the inner structure is similar to the other investigated cactus species. The parenchymatous pith in a branchless region is surrounded by a vascular tube (figure 1*f*), whereas in the junction zone, a compact wood socket connects the vascular tissue of branch and stem (figure 2*l*).

### (b) Material properties

Pith and cortex of all investigated species showed a progressively nonlinear stress–strain behaviour (figure 3*a*), whereas the skin featured a regressive behaviour (figure 3*b*). The wood samples initially showed in good approximation a linear elastic behaviour with a slight divergence at higher strains (figure 3*b*). Table 1 summarizes the arithmetic mean

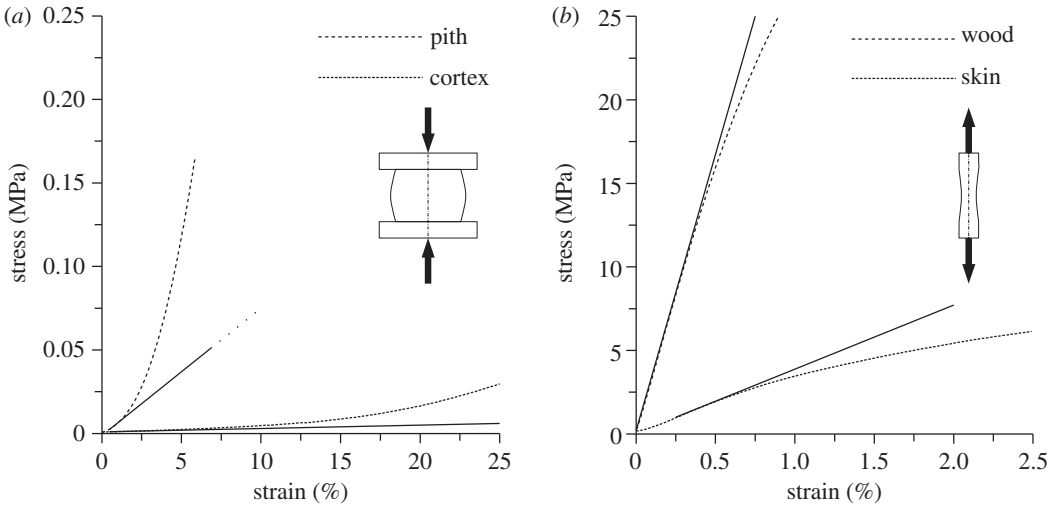


**Figure 3.** (*a*) Representative stress–strain curves for uniaxial compression tests of pith and cortex parenchyma. (*b*) Representative stress–strain curves for uniaxial tension tests of wood and skin samples. The slope of the linear regression lines (straight continuous lines) represents the Young modulus.

**Table 1.** Young's moduli in cactus stems depending on the tissue and the species. *E*, Young's modulus (arithmetic mean value ± s.d.); *N*, number of the tested specimens; *P*, probability value (*p*-value) from the Kruskal–Wallis one-way analysis of variance by ranks (KW test). $P_{all}$, overall comparison; $P_{hth}$, head-to-head record; $_{P-C}$, between *P. pachycladus* and *C. morawetzianus*; $_{C-M}$, between *C. morawetzianus* and *M. geometrizans*; $_{M-P}$, between *M. geometrizans* and *P. pachycladus*.

| species | $E_{pith}$ (MPa)[a] | *N* | $E_{wood}$ (MPa)[b] | *N* | $E_{cortex}$ (MPa)[a] | *N* | $E_{skin}$ (MPa)[b] | *N* | $P^c_{all}$ |
|---|---|---|---|---|---|---|---|---|---|
| *Pilosocereus pachycladus* | 0.78 ± 0.40 | 16 | 3173.6 ± 599.8 | 6 | 0.02 ± 0.01 | 22 | 373.2 ± 38.1 | 5 | $<10^{-8}$ |
| $P^d_{hth,\ P-C}$ | $<10^{-4}$ | | $<10^{-2}$ | | $<10^{-5}$ | | $<10^{-3}$ | | |
| *Cleistocactus morawetzianus* | 0.10 ± 0.07 | 10 | 1218.9 ± 222.1 | 8 | 0.77 ± 0.23 | 10 | 213.8 ± 59.1 | 8 | $<10^{-6}$ |
| $P^d_{hth,\ C-M}$ | 0.725 | | $<10^{-3}$ | | $<10^{-3}$ | | $<10^{-2}$ | | |
| *Myrtillocactus geometrizans* | 0.12 ± 0.07 | 11 | 3148.0 ± 649.7 | 8 | 0.04 ± 0.01 | 8 | 566.8 ± 92.1 | 8 | $<10^{-5}$ |
| $P^d_{hth,\ M-P}$ | $<10^{-4}$ | | 0.606 | | <0.05 | | $<10^{-2}$ | | |
| $P^d_{all}$ | $<10^{-5}$ | | $<10^{-3}$ | | $<10^{-5}$ | | $<10^{-3}$ | | |

[a]Uniaxial compression test.
[b]Uniaxial tension test in longitudinal direction.
[c]Intraspecific.
[d]Interspecific.

values and the standard deviations for the Young's moduli of the different tissues. In addition, the probability values (*p*-values) for the overall interspecific and intraspecific Kruskal–Wallis (KW) one-way analysis of variance by ranks (KW test) [16] as well as the interspecific head-to-head records are listed. All except three of them lie in the range from $10^{-8}$ up to $10^{-2}$. The exceptions are the head-to-head records of the Young's moduli for the pith of *C. morawetzianus* and *M. geometrizans* with a *p*-value of 0.725, for the wood of *M. geometrizans* and *P. pachycladus* with a *p*-value of 0.606, and for the cortex of *M. geometrizans* and *P. pachycladus* with a *p*-value close to 0.05 (cf. table 1). The *p*-values of the intraspecific head-to-head records are not displayed in table 1. All except one of them lie in the range from $10^{-7}$ up to $10^{-2}$. The exception is the head-to-head record of the Young's moduli for the pith and the cortex parenchyma of *M. geometrizans* with a *p*-value close to 0.05.

## (c) Results of the finite-element analysis

### (i) Reference model

The reference model of two joint cylindrical tubes shows the typical stress distribution of a cantilever beam under self-loading conditions (figure 4*c*,*g*). Tension stresses on the adaxial and compression stresses on the abaxial side of the branch reach their maxima at the junction of the branch with the stem. The sharp edge at the transition leads to a very high stress concentration (notch stresses, arrows in figure 4*c*,*g*), which increases the risk of failure [5,10,11].

### (ii) The Mattheck model

In a model based on the design rules proposed by Mattheck [5,10,11], the mechanical stresses in the junction zone are spread over a larger area (compare figure 4*d*,*h* with figure 4*c*,*g*). The enlarged branch base diameter in combination with a

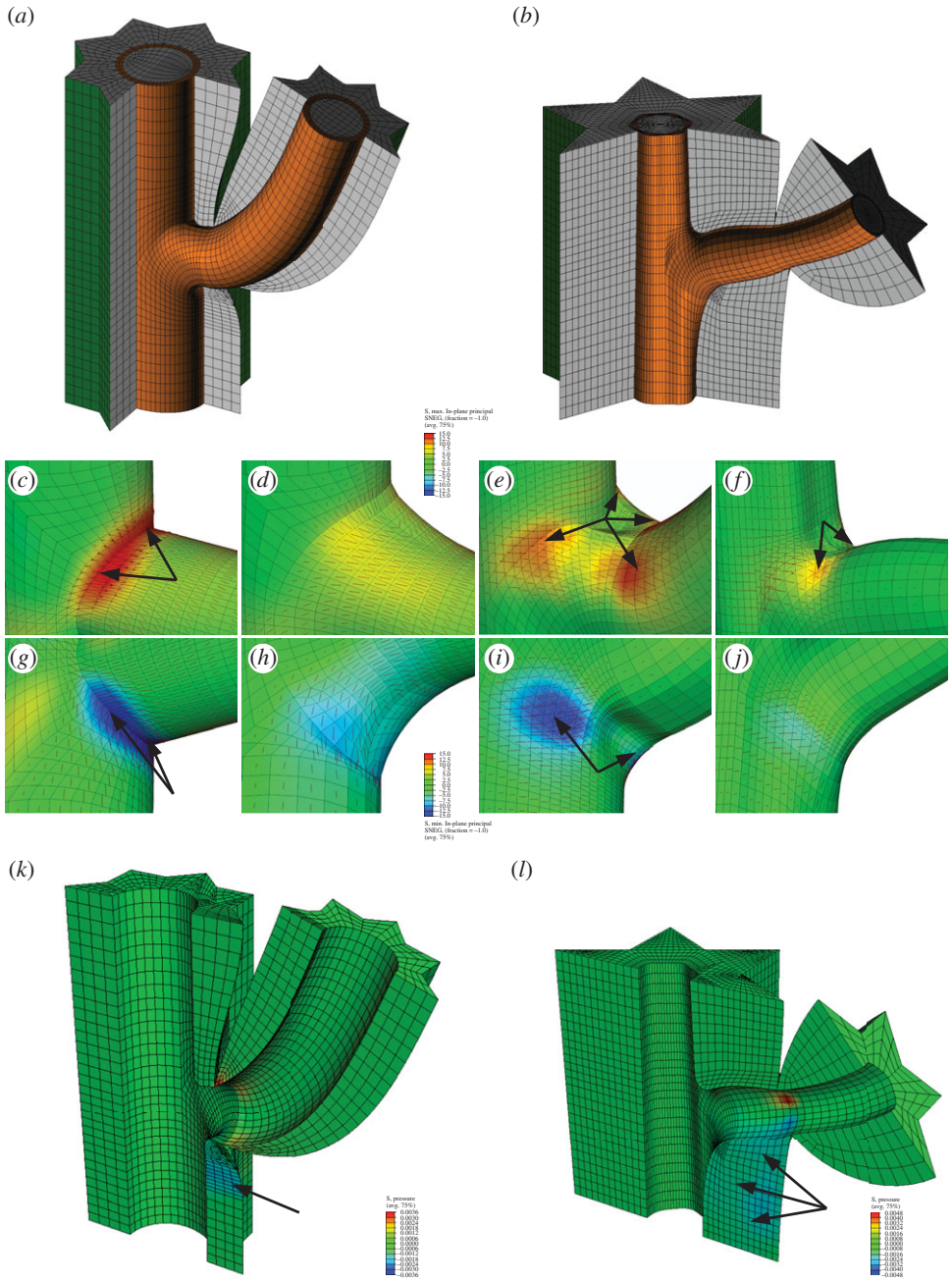


**Figure 4.** Finite-element analysis (FEA) of ramification models. Entire finite-element models of (*a*) *Pilosocereus pachycladus* and (*b*) *Myrtillocactus geometrizans*. Stress distribution in the vascular tissue: tension stresses (red) on the adaxial side (*c*–*f*) and compression stresses (blue) on the abaxial side (*g*–*j*) of the ramification of (*c*,*g*) a reference model consisting of two joint cylindrical tubes; (*d*,*h*) a model according to methods developed by Mattheck [5,10,11]; (*e*,*i*) the model of *P. pachycladus;* and (*f*,*j*) the model of *M. geometrizans*. Compression stress distribution (blue) in the succulent cortex: (*k*) model of *P. pachycladus;* (*l*) model of *M. geometrizans*. Arrows: (*c*,*g*) stress maxima; (*e*,*f*) lateral shift of the tension stress maxima; (*i*) lateral shift of the compression stress maxima; (*k*,*l*) compression stress in the cortex on the abaxial side of the ramification.

smooth curvature in the transition zone between stem and branch helps to reduce the stress magnitude and lead to a homogeneous stress distribution with no critical notch stress peaks on the abaxial and adaxial side of the branch base.

### (iii) *Pilosocereus pachycladus*

The model representing the lignified vascular support structure of the ramification of *P. pachycladus* shows that the indentations on the adaxial and abaxial side in combination with the orthotropic material behaviour divide the stress maxima in two major parts and shift them laterally towards the periphery of the branch socket (compare figure 4*e*,*i* with figure 4*c*,*g*). No critical stress concentrations can be found in the median regions. In simulations that also take the succulent cortex into account a reduction of the compression stress in the vascular tissue on the abaxial side of the branch base could be detected as the succulent cortex partly dissipates the compression stress (arrow in figure 4*k*).

### (iv) *Cleistocactus morawetzianus*

The branching is morphologically very similar to *P. pachycladus*, suggesting that the results are transferable to *C. morawetzianus*. Therefore, no additional simulation was performed.

### (v) *Myrtillocactus geometrizans*

The simulation excluding the cortex features a homogeneous stress distribution with no stress concentrations on the

abaxial side of the ramification similar to the Mattheck model (compare figure 4*j* with figure 4*h*). On the adaxial side, the orthotropic material behaviour of the cactus wood leads to a lateral shift of the stress maximum. The median section is free of tension stresses. The difference from a 'normal' tree ramification is substantiated in simulations including the cortex. The tension stress maxima and compression stress minima in the vascular tissue are reduced by almost 50%. The cortex partly dissipates the compression stress on the abaxial side of the branch (arrows in figure 4*l*).

## 4. Discussion

### (a) Material properties

Owing to the small sample size available for material testing, the reliability of the presented results is limited, but still sufficiently detailed to allow for comparative studies among the considered species, as well as between columnar cacti and other arborescent dicotyledons with lignified supporting tissue.

The fact that all investigated plants were raised in greenhouses without wind loads and their young age in comparison with fully grown cacti in their natural habitat reduces the validity of the results to young plants. However, structure–function relationships between the mechanical properties of the constituent tissues and the (shrubby or tree-like) habit can be observed.

The nonlinear stress–strain behaviour of pith and cortex in all investigated specimens (figure 3*a*) is typical for nonlinear elastic materials under compression [17], whereas the stress–strain curve of the skin with a divergence at higher strains (figure 3*b*) is typical for a nonlinear elastic material under tensile load. The values confirm former results for the skin of other cactus species [18]. The initial linear elastic behaviour of wood with a slight divergence at higher strains (figure 3*b*) is similar to hardwood known in other dicotyledons [19].

The intraspecific comparison of the Young's moduli of the different cactus tissues confirms the assumption that the cactus wood represents the main mechanical support of the ramification (cf. table 1 [4]).

The rather low Young's moduli in longitudinal direction of the cactus woods in comparison with other diffuse porous hardwoods such as paper birch (*Betula papyrifera*, $E = 8100$ MPa) [19] or silver maple (*Acer saccharinum*, $E = 6500$ MPa) [19] correlate with the large multi-seriate rays, which reduce the relative amount of stiff fibres in longitudinal direction of the vascular tissue (figure 1*g–l* [20]).

For both tree-like species *P. pachycladus* and *M. geometrizans*, the Young's moduli of wood and pith are significantly higher than in the shrubby *C. morawetzianus*. This difference is also expressed by the response upon drought: while the branches of the tree-like species remain in their positions, the arch-shaped, slender shoots of *C. morawetzianus* bend down under water stress, suggesting that the stability of its branches relies on a hydraulic system consisting of the wood, the peripheral cortex and the skin. The low Young's modulus of the pith of *C. morawetzianus* and the presence of horizontal growth ruptures reduces its contribution to mechanical stability. It seems that during drought and the concomitant diminished water content, the turgor pressure of the parenchymatous cortex cells drops, and therefore the stiffening effect of the cortex is reduced. The hydraulic system collapses and the shoots bend down. By contrast, the pith of the two tree-like cacti *P. pachycladus* and *M. geometrizans* exhibits higher Young's moduli than their cortex. This finding points to a mechanism that helps decreasing the buckling risk of the cactus shoots in younger stages (when the wall thickness of the vascular tube is still small) by preventing an ovalization of the wall of the vascular cylinder [21–23].

### (b) Stress–strain relationships in branch–stem attachment

Prerequisite for understanding the load adaptation in cactus ramifications is the theorem of collinearity between fibre course and main tension stress direction. Owing to their flexibility, individual fibres are good at tolerating tension forces but very poor at resisting compression stresses. Therefore, in a composite material (such as the vascular tissue of plants), the fibres ideally should be arranged according to the tension stress direction; that is, in a horizontally oriented cantilevered beam under dead-weight conditions, the fibres lie on the upper (adaxial) side of the beam in longitudinal direction [2]. Embedding the fibres in a compression-stiff matrix material (lignification of the cell walls of the vascular tissue) allows it to deal with compression stresses on the lower (abaxial) side. Additionally, tree ramifications feature characteristic shapes at the branch–stem junction resulting from material accumulation by secondary growth. This leads to homogeneous stress conditions with no critical notch stresses at the transition to the stem (figure 4*d*,*h* [5,10,11]).

The load adaptation of *M. geometrizans* follows this rule to some extent. The dissected specimens closely resemble typical hardwood tree ramifications. This is mirrored by the finite-element analysis results of the simulation excluding the cortex. As in deciduous trees, the stress maxima are spread over a larger area when compared with the reference model (compare figure 4*f*,*j* with figure 4*c*,*g*); but the secondary growth still remains limited by the surrounding cortex. So it is likely that the broad parenchymatous cortex itself takes over the role as mechanical support (arrows in figure 4*l*).

In contrast to *M. geometrizans*, *P. pachycladus* does not exhibit such a thick cortex when compared with the dimensions of the vascular tissue (compare figure 1*d* with figure 1*f*). The secondary growth of the wood is even more constrained, resulting in a differing load adaptation of the vascular tissue in the ramification zone. Under the above-mentioned precondition of stress and fibre collinearity, the abaxial and adaxial median regions feature distinct indentations that divide the central stress maxima (compare figure 4*e*,*i* with figure 4*c*,*d*). Owing to the orthotropic material behaviour of the wood, the stress concentrations are shifted laterally towards regions with a smooth curvature between stem and branch, where the fibre course exhibits no abrupt change of direction. As a result, all fibres are aligned according to the tension stress direction.

## 5. Conclusion and outlook

Load adaptation in ramifications of columnar cacti takes place on different hierarchical levels by fine-tuning the fibre orientations in the cactus wood according to the stresses and the stress directions. On a macroscopic scale (= organ level), the shape of the branch socket modifies the predominant stresses in a way that the re-oriented tension stress trajectories better

match already existing fibre orientations running from the stem into the branch. The thickness of the vascular tissue in the stem below a ramification increases to support the additional weight of the branch as well as to ensure the water supply of the branch. At tissue level, there is a higher number of interconnections between the wood lamellae in the branching region. The alignment of these interconnections reflects the orientation of the stress trajectories between branch and stem. It is also likely that load adaptation of the different tissues takes place at cellular or cell wall level, but up to now, this has not been analysed. In addition, in columnar cacti, the formation of tension wood in regions of high-tension stresses, typical of angiosperm trees, remains unclear. In order to shed light on these open questions, the mechanical role of the parenchymatous pith and cortex have to be reconsidered, and the interaction between the different tissues on all hierarchical levels has to be analysed. This will provide an even better understanding of the functional anatomy and biomechanics of columnar cacti.

Consequently, for further investigations, the biomechanical models have to be improved significantly by using accurate imaging techniques such as microfocus computed tomography. The obtained three-dimensional voxel images might be transformed by reverse engineering techniques to finite-element models already incorporating the fibre course of the cactus wood. The necessary orthotropic material properties for these models should be assessed in mechanical tests with external (e.g. optical) strain measurement devices to allow for determining Young's modulus as well as Poisson's ratio at the same time.

The described load adaptation strategy in cacti finally may serve as a model for bioinspired technical components in lightweight engineering. As the design space is often limited, there is a high market potential for innovative fibre-composite components with slim outer contours. Promising applications (e.g. in automotive engineering) are highly loaded nodal elements (such as forks, steering heads, wheel suspensions, axle carriers, etc.) that can be produced as carbon-fibre composite constructions to substitute for steel or aluminium as basic materials.

Acknowledgements. We thank Dipl.-Ing. (FH) Andreas Freund from the Institute for Lightweight Engineering and Polymer Technology (ILK) at the TU Dresden for valuable help in developing the finite-element models.

Funding statement. The authors gratefully acknowledge the funding of the study by the German Research Foundation (DFG) within the Priority Programme SPP 1420 'Biomimetic materials research: functionality by hierarchical structuring of materials'.

## References

1. Mauseth JD, Kiesling R, Ostolaza C. 2002 *A cactus odyssey*. Portland, OR: Timberpress.
2. Klein B. 2005 *Leichtbau-Konstruktion*, 6th edn. Wiesbaden, Germany: Vieweg.
3. Mauseth JD. 2006 Structure–function relationships in highly modified shoots of Cactaceae. *Ann. Bot.* **98**, 901–926. (doi:10.1093/aob/mcl133)
4. Niklas KJ, Molina-Freaner F, Tinoco-Ojanguren C. 1999 Biomechanics of the columnar cactus *Pachycereus pringlei*. *Am. J. Bot.* **86**, 767–775. (doi:10.2307/2656697)
5. Mattheck C. 1990 Design and growth rule for biological structures and their application in engineering. *Fatigue Fract. Eng. Mater. Struct.* **13**, 535–550. (doi:10.1111/j.1460-2695.1990.tb00623.x)
6. Müller U, Gindl W, Jeronimidis G. 2006 Biomechanics of a branch–stem junction in softwood. *Trees* **20**, 643–648. (doi:10.1007/s00468-0060079-x)
7. Shigo AL. 1985 How tree branches are attached to trunks? *Can. J. Bot.* **63**, 1391–1401. (doi:10.1139/b85-193)
8. Speck T, Burgert I. 2011 Plant stems: functional design and mechanics. *Annu. Rev. Mater. Res.* **41**, 169–193. (doi:10.1146/annurev-matsci-062910-100425)
9. Niklas KJ. 1992 *Plant biomechanics: an engineering approach to plant form and function*. Chicago, IL: University of Chicago Press.
10. Mattheck C. 1998 *Design in nature: learning from trees*. Heidelberg, Germany: Springer.
11. Mattheck C. 2006 *Design in der Natur: Der Baum als Lehrmeister*, 4th edn. Freiburg, Germany: Rombach.
12. Bobich EG, Nobel PS. 2001 Biomechanics and anatomy of cladode junctions for two *Opuntia* (Cactaceae) species and their hybrid. *Am. J. Bot.* **88**, 391–400. (doi:10.2307/2657103)
13. Anderson EF. 2001 *The cactus family*. Portland, OR: Timber Press.
14. Hunt DR. 2006 *The new cactus lexicon*. Milborne Port, UK: DH Books.
15. Riehle M, Simmchen E. 2000 *Grundlagen der Werkstofftechnik*, 2nd edn. Stuttgart, Germany: Deutscher Verlag für Grundstoffindustrie.
16. Kruskal WH, Wallis AW. 1952 Use of ranks in one-criterion variance analysis. *J. Am. Stat. Asssoc.* **47**, 583–621. (doi:10.1080/01621459.1952.10483441)
17. Fung YC. 1984 Structure and stress–strain relationship of soft tissues. *Am. Zool.* **24**, 13–22.
18. Bargel H. 2005 *Biomechanical properties of the plant cuticle and its possible role as a structural stabilisation component*. Dresden, Germany: TU Dresden.
19. Kretschmann DE. 2010 Mechanical properties of wood. In *Wood handbook: wood as an engineering material* (ed. Forest Products Laboratory), pp. 5-1–5-46. Madison, WI: Forest Service.
20. Wagner ST, Isnard S, Rowe NP, Samain M-S, Neinhuis C, Wanke S. 2012 Escaping the Lionoid habit: evolution of shrub-like growth forms in *Aristolochia* subgenus *Isotrema* (Aristolochiaceae). *Am. J. Bot.* **99**, 1609–1629. (doi:10.3732/ajb.1200244)
21. Rowe NP, Isnard S, Speck T. 2004 Diversity of mechanical architectures in climbing plants: an evolutionary perspective. *J. Plant Growth Regul.* **23**, 108–128. (doi:10.1007/s00344-004-0044-0)
22. Spatz H-CH, Köhler L, Speck T. 1998 Biomechanics and functional anatomy of hollow stemmed sphenopsids: I. *Equisetum giganteum*. *Am. J. Bot.* **85**, 305–314. (doi:10.2307/2446321)
23. Speck T, Speck O, Emanns A, Spatz H-CH. 1998 Biomechanics and functional anatomy of hollow stemmed sphenopsids: III. *Equisetum hyemale*. *Bot. Acta* **111**, 366–376.